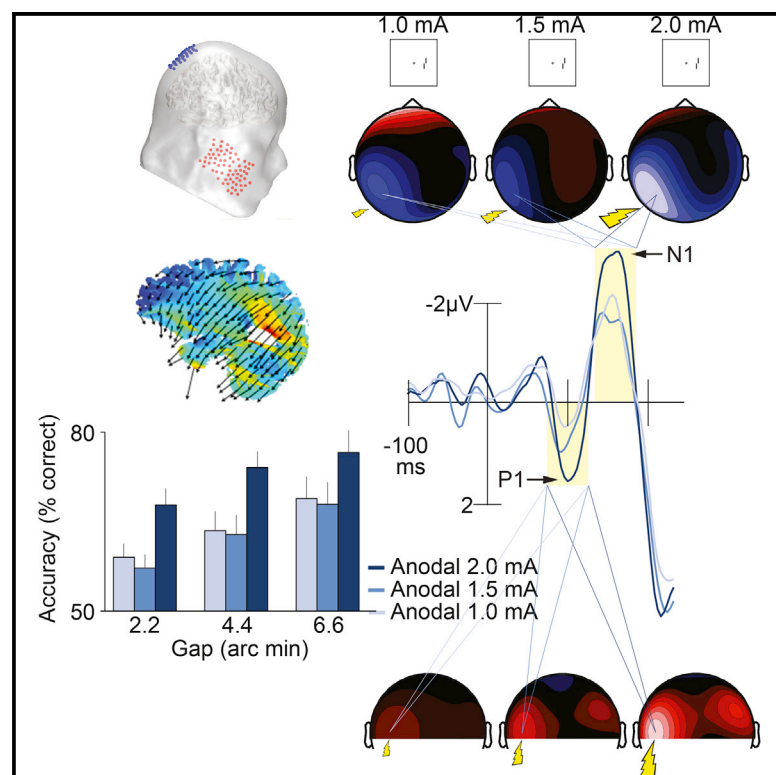


Current Biology

Electrical Stimulation of Visual Cortex Can Immediately Improve Spatial Vision

Graphical Abstract



Authors

Robert M.G. Reinhart, Wenxi Xiao,
Laura J. McClenahan, Geoffrey F.
Woodman

Correspondence

geoffrey.f.woodman@vanderbilt.edu

In Brief

Reinhart et al. show that 20 min of direct-current stimulation can change visual acuity. Subjects' event-related potentials showed the same pattern of amplitude changes observed with behavior. Finally, subjects with the worst visual acuity showed the largest improvements following anodal stimulation of visual cortex.

Highlights

- Twenty minutes of direct-current stimulation improved visual acuity by ~15%
- Stimulation changed the amplitude of visually evoked potentials
- Subjects with the lowest acuity benefited the most from stimulation



Electrical Stimulation of Visual Cortex Can Immediately Improve Spatial Vision

Robert M.G. Reinhart,¹ Wenxi Xiao,² Laura J. McClenahan,² and Geoffrey F. Woodman^{2,*}

¹Department of Psychological and Brain Sciences, Boston University, Boston, MA 02215, USA

²Department of Psychology, Center for Integrative and Cognitive Neuroscience, Vanderbilt Vision Research Center, Vanderbilt University, Nashville, TN 37240, USA

*Correspondence: geoffrey.f.woodman@vanderbilt.edu

<http://dx.doi.org/10.1016/j.cub.2016.05.019>

SUMMARY

We can improve human vision by correcting the optics of our lenses [1–3]. However, after the eye transduces the light, visual cortex has its own limitations that are challenging to correct [4]. Overcoming these limitations has typically involved innovative training regimes that improve vision across many days [5, 6]. In the present study, we wanted to determine whether it is possible to immediately improve the precision of spatial vision with noninvasive direct-current stimulation. Previous work suggested that visual processing could be modulated with such stimulation [7–9]. However, the short duration and variability of such effects made it seem unlikely that spatial vision could be improved for more than several minutes [7, 10]. Here we show that visual acuity in the parafoveal belt can be immediately improved by delivering noninvasive direct current to visual cortex. Twenty minutes of anodal stimulation improved subjects' vernier acuity by approximately 15% and increased the amplitude of the earliest visually evoked potentials in lockstep with the behavioral effects. When we reversed the orientation of the electric field, we impaired resolution and reduced the amplitude of visually evoked potentials. Next, we found that anodal stimulation improved acuity enough to be measurable with the relatively coarse Snellen test and that subjects with the poorest acuity benefited the most from stimulation. Finally, we found that stimulation-induced acuity improvements were accompanied by changes in contrast sensitivity at high spatial frequencies.

RESULTS

In experiment 1, we stimulated posterior visual cortex (i.e., occipitoparietal cortex) with transcranial direct-current stimulation (tDCS). We parametrically manipulated stimulation intensity to determine what dose might improve visual-spatial precision. All 20 subjects completed three anodal stimulation conditions at varying stimulation intensities (1.0, 1.5, and 2.0 mA) on different days, with the order randomized across subjects. We stimulated

either the left or right hemisphere (see Figure 1A; hemisphere counterbalanced), with stimuli presented in the stimulated visual field (i.e., contralateral [contra]) or the unstimulated visual field (i.e., ipsilateral [ipsi]), similar to approaches in neuropsychology [11]. We used 20 min of anodal tDCS in each condition because this duration and current-flow direction have been shown to increase neuronal excitability [7, 12–15]. Subjects were blind to the stimulation conditions, as verified with debriefing questionnaires (see the Supplemental Experimental Procedures).

Immediately following stimulation, subjects performed a lateralized version of the vernier acuity task (Figure 1B). Subjects judged the relative position of two abutting vertical lines and indicated whether the upper line was displaced to the left or right of the lower line, displaced by 2.2, 4.4, or 6.6 arc min randomized across trials, with the lines centered 5° to the left or right of fixation [16–18] (i.e., in the parafoveal belt; see the Supplemental Experimental Procedures for details). This combination of eccentricity and displacement was sufficient to bring subjects' performance below ceiling and reveal stimulation benefits if they existed.

Experiment 1 showed that 20 min of anodal stimulation at 2.0 mA improved vernier acuity relative to performance following 1.0 and 1.5 mA of stimulation. Figures 1C and 1D show that we found significant main effects of intensity on reaction time (RT) ($p = 0.01$) and accuracy ($p = 0.04$) across task difficulty levels (2.2–6.6 arc min) (see Table S1 for statistical details). These main effects were due to 2.0 mA resulting in faster RTs and higher accuracy than 1.0 mA (RT, $p = 0.01$; accuracy, $p = 0.04$) and 1.5 mA of tDCS (RT, $p = 0.02$; accuracy, $p = 0.03$). However, this was only true for stimuli presented contralateral to the stimulating electrode. For ipsilateral stimuli, the stimulation intensity had no significant behavioral effects (RT, $p = 0.64$; accuracy, $p = 0.91$). These lateralized improvements did not differ between subjects who received left- versus right-hemisphere tDCS (no stimulation location \times intensity interactions on RT, contra, $p = 0.93$; ipsi, $p = 0.25$; or accuracy, contra, $p = 0.79$; ipsi, $p = 0.95$). These findings show that increasing the excitability of visual cortex with anodal direct current can improve behavioral measures of vernier acuity in the parafovea.

By recording the subjects' event-related potentials (ERPs), we verified that stimulation was changing how the brain processed the visual information at the earliest measurable points in processing. Figures 1E–1G show that the stimulation enhanced the early visual waveforms related to sensory processing (i.e., the visual first positive component [P1] and first negative component [N1]) [19]. The P1 and N1 amplitudes elicited by stimuli

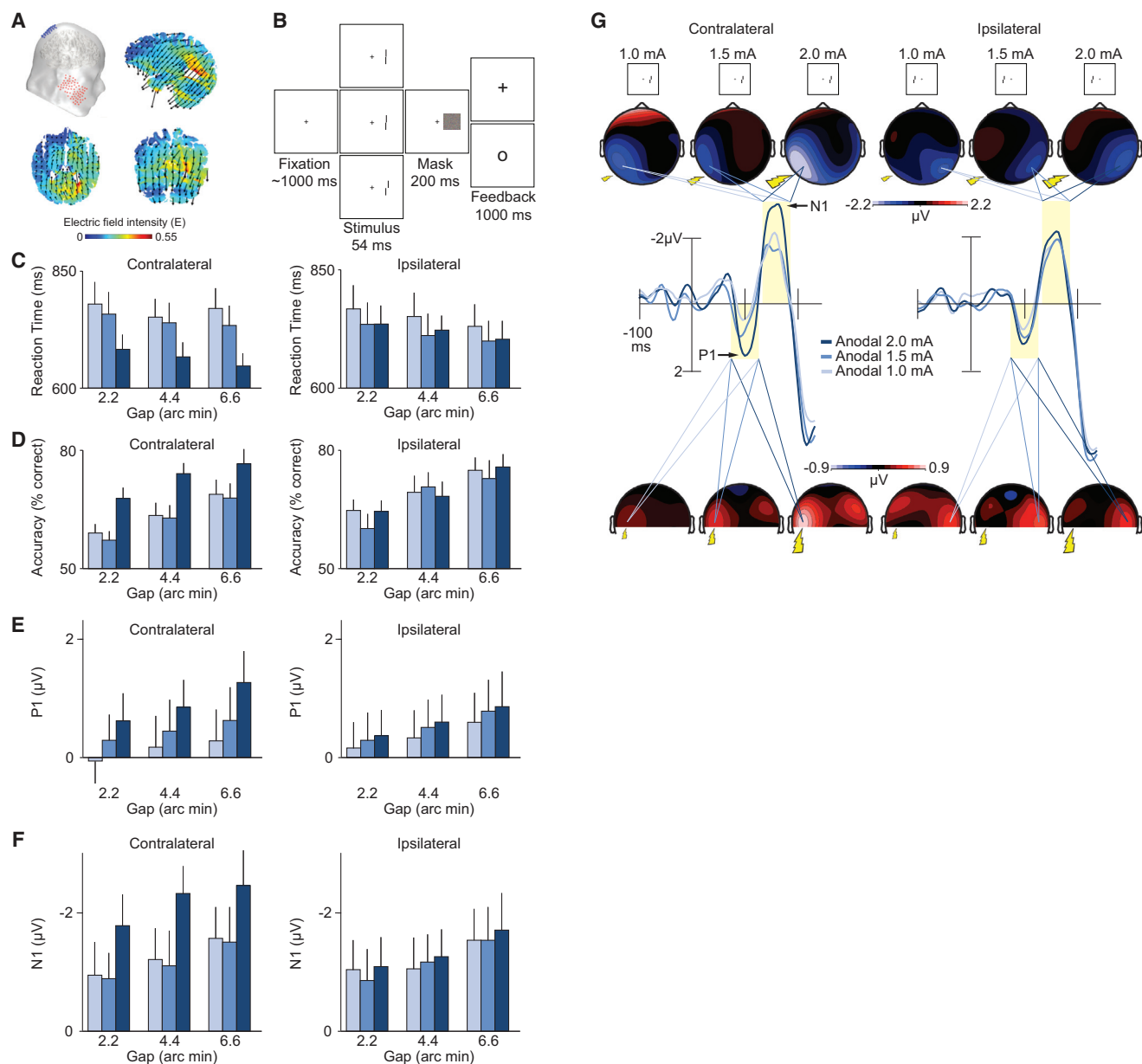


Figure 1. Current-Flow Model, Task, and Results from Experiment 1

(A) Our visual cortex transcranial direct-current stimulation (tDCS) montage with the anode over site P1 or P2 and cathode over the left or right cheek, respectively. The schematic shows the P2 (anodal) and right cheek (reference) configuration. Sagittal, axial, and coronal maps centered on the gravity center of the induced electric field show current flow through the brain. Arrows show the orientation of the electric field. Warmer colors show greater electric field magnitude.

(B) The vernier acuity task requiring subjects to judge the relative position of two line segments in the periphery while maintaining central fixation. Subjects indicated with one of two buttons on a game pad whether the upper line was offset to the left or right of the lower line.

(C and D) Mean correct reaction time (RT) (C) and accuracy (D) across offset size (2.2, 4.4, 6.6 arc min) and tDCS intensity level (1.0, 1.5, 2.0 mA). Data are binned according to the location of vernier stimuli with respect to tDCS application (contralateral, ipsilateral). For example, contralateral data include trials with left visual field stimuli following right-hemisphere tDCS, and trials with right visual field stimuli following left-hemisphere tDCS. See also Figure S1 for accuracy across the entire experimental session and Figure S2 for how this performance is related to improvements in contrast sensitivity.

(E and F) Mean amplitude of the P1 (E) and N1 (F) event-related potentials (ERPs) as in (C) and (D).

(G) Waveforms time locked to the onset of the vernier stimuli and related topographical maps across tDCS and laterality conditions. Shaded regions show the analysis windows for the P1 (75–125 ms) and N1 (140–190 ms) component amplitudes. Topographies show data collapsed across vernier stimulus locations and the hemispheres of tDCS application using a method that preserved the electrode location relative to the location of the stimuli. All contralateral signals are projected onto the left hemisphere (contralateral), and ipsilateral signals are projected onto the right hemisphere (ipsilateral). Error bars show the SEM in this and all subsequent figures. See also Table S1 for the results of the statistical analyses in their entirety.

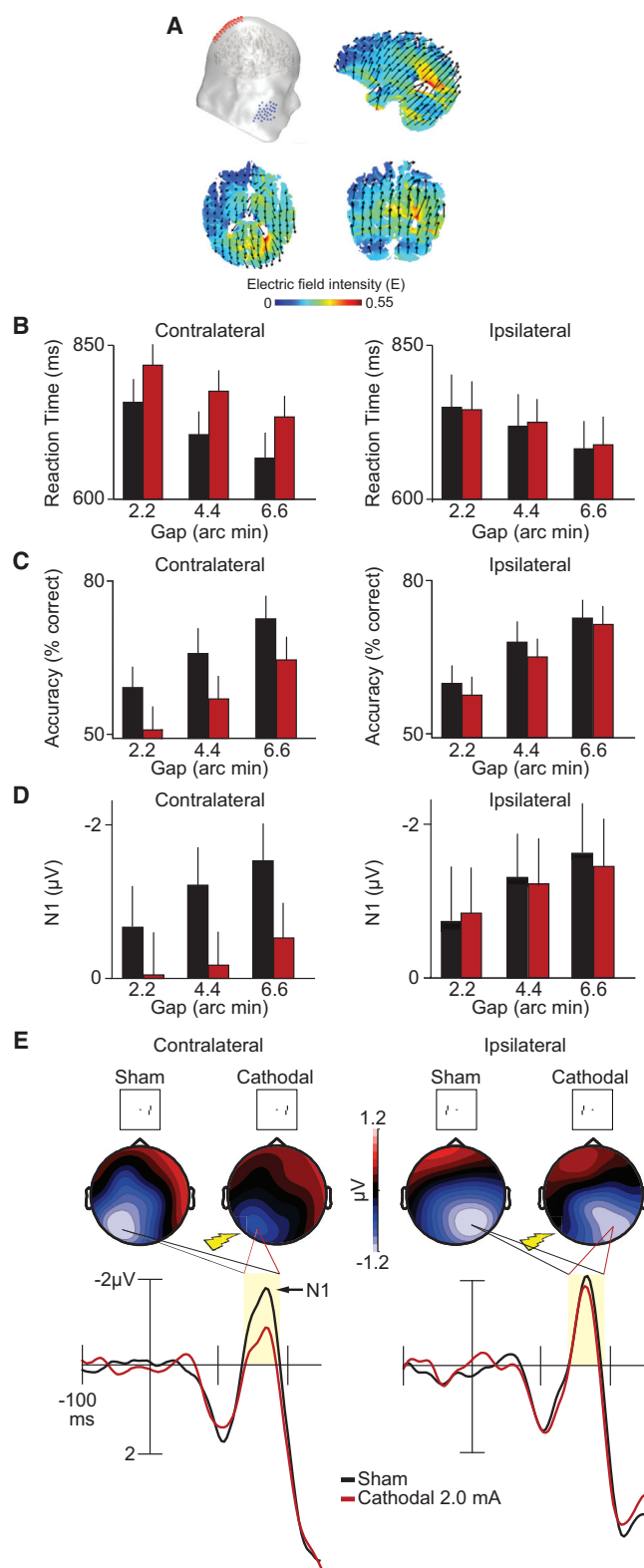


Figure 2. Current-Flow Model and Results from Experiment 2

(A) Our visual cortex tDCS montage used a cathodal electrode over the P1 or P2 site (International 10–20 System) paired with an anodal electrode over the left or right cheek, respectively. The schematic here shows the P2 (cathodal) and right cheek (reference) configuration. Sagittal, axial, and coronal maps

contralateral to the stimulation increased with intensity (main effect of intensity on P1, $p = 0.05$; N1, $p = 0.01$), with the strongest enhancements following 2.0 mA relative to 1.0 mA intensity (P1, $p = 0.04$; N1, $p = 0.01$). No stimulation-induced changes to P1 and N1 amplitudes were observed for ipsilaterally presented stimuli (P1, $p = 0.61$; N1, $p = 0.90$) or between lower stimulation intensities (1.0 mA versus 1.5 mA, P1 contra, $p = 0.22$; P1 ipsi, $p = 0.50$; N1 contra, $p = 0.76$; N1 ipsi, $p = 0.91$). Thus, the subjects' visual P1 and N1 components exhibited amplitude changes that mirrored the behavioral effects, demonstrating that tDCS changed the earliest stages of processing in the visual system.

Our results from experiment 1 show that the benefits of anodal stimulation over visual cortex were only evident when we used 2.0 mA of tDCS for 20 min, not the lower levels of intensity. In our subsequent experiments, we focused on this level of current in our active stimulation conditions.

Next, we reversed the direction of current flow in experiment 2 (Figure 2A). All subjects completed a sham baseline condition and an active 2.0 mA cathodal stimulation condition on different days, with the order counterbalanced across subjects. Cathodal stimulation has been shown to decrease the excitability of cortex in humans and animal models [12, 20]. Thus, 20 min of cathodal stimulation should decrease vernier acuity and reduce the amplitude of the visual ERPs relative to the sham baseline.

Experiment 2 demonstrated that we could push behavior and the subjects' visual ERPs in the opposite direction with cathodal tDCS. Figures 2B and 2C show that relative to the sham baseline condition, 20 min of 2.0 mA cathodal tDCS significantly slowed RTs ($p = 0.03$) and reduced accuracy ($p = 0.04$) across displacements (i.e., 2.2–6.6 arc min) (see Table S1 for statistical details). These behavioral changes in vernier acuity were specific to the visual field contralateral to the tDCS. No such changes in task performance were observed for ipsilaterally presented stimuli (RT, $p = 0.95$; accuracy, $p = 0.48$).

Figures 2D and 2E show that cathodal stimulation reduced the amplitude of the visual N1 component relative to sham, but this time largely spared the amplitude of the preceding P1 component. Paralleling the behavior, we found a spatially mapped pattern of ERP results. Only N1 amplitudes elicited by stimuli appearing contralateral to the tDCS were significantly reduced (contra, $p = 0.03$; ipsi, $p = 0.87$). No effects were seen in the P1 amplitude following stimulation (contra, $p = 0.23$; ipsi, $p = 0.89$). The findings of experiment 2 demonstrate that by

centered on the gravity center of the induced electric field show current flow through the brain. Arrows denote the orientation of the electric field, and warmer colors denote greater electric field magnitude.

(B and C) Mean correct RT (B) and accuracy (C) for vernier offset discrimination as a function of gap offset size (2.2, 4.4, 6.6 arc min) and tDCS condition (sham, black; 2.0 mA cathodal, red). Data are sorted by the location of the vernier stimuli with respect to tDCS application (contralateral, ipsilateral) as in Figure 1.

(D) Mean N1 amplitude as in (B) and (C).

(E) Waveforms time locked to the onset of the vernier stimuli and related topographies across tDCS and laterality conditions. The arrow indicates the N1 component. Shaded regions show the analysis window for the N1 component amplitude (140–190 ms). Topographies show all contralateral and ipsilateral signals as described in Figure 1G.

See also Table S1 for the results of the statistical analyses in their entirety.

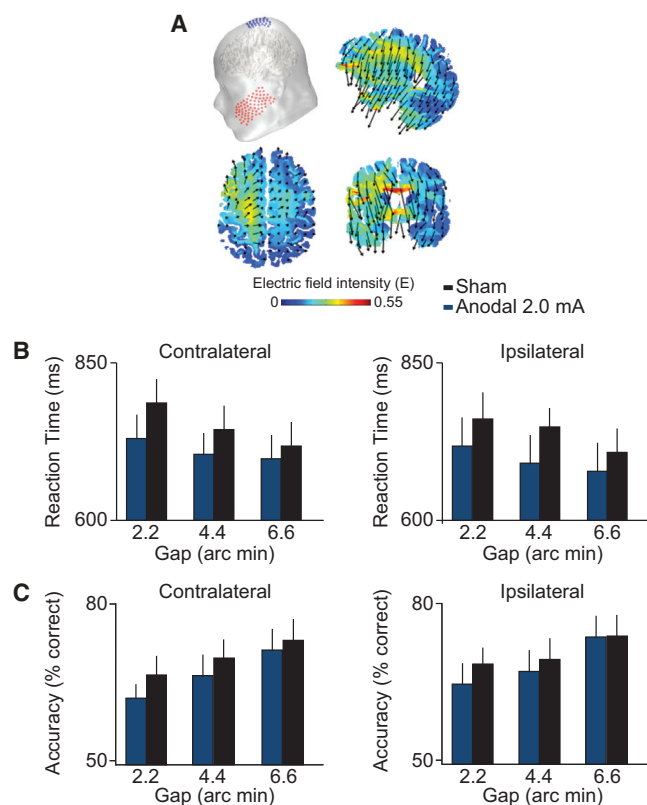


Figure 3. Current-Flow Model and Results from Experiment 3

(A) Our motor cortex tDCS montage used an anodal electrode over the C1 or C2 site (central 1 and 2 electrodes in the 10/20 system) paired with a cathodal electrode over the left or right cheek, respectively. The schematic shows the C1 (anodal) and left cheek (cathodal) configuration. Sagittal, axial, and coronal maps centered on the gravity center of the induced electric field show current flow through the brain. Arrows denote the orientation of the electric field, and warmer colors denote greater electric field magnitude.

(B and C) Mean correct RT (B) and accuracy (C) for the vernier stimuli as a function of gap offset size (2.2, 4.4, 6.6 arc min) and tDCS condition (sham, 2.0 mA anodal). Data are sorted by laterality (contralateral, ipsilateral) as in Figures 1 and 2.

reversing the current flow, we can flip the behavioral and electrophysiological effects that we observed in experiment 1.

If the results from experiments 1 and 2 are not unique to tDCS applied to visual cortex but can be produced using any lateralized tDCS montage due to nonspecific effects such as arousal or demand characteristics, then we should find a similar pattern of results when stimulating over a different brain region. In experiment 3, we applied 20 min of sham and 2.0 mA anodal tDCS over the left or right hemisphere of motor cortex (see Figure 3A), with the hemisphere counterbalanced across 20 subjects, prior to having the subjects complete the vernier acuity task. These subjects showed a completely different pattern of behavioral effects compared to tDCS of visual cortex. Figures 3B and 3C show that subjects simply responded faster and less accurately regardless of the location of stimuli in the visual field (see the Supplemental Results and Discussion for details). Whereas the results of experiments 1 and 2 rule out attentional, eye movement, and pupil dilation accounts of the tDCS effects (see the Supplemental Re-

sults and Discussion for details), the results of experiment 3 show that only tDCS of visual cortex improves performance in the vernier task.

If the anodal stimulation of experiment 1 is truly improving subjects' visual-spatial resolution, then we should improve real-world acuity outside the laboratory. In experiment 4, we examined the impact of 20 min of 2.0 mA anodal tDCS of visual cortex on the performance of the Snellen chart for visual acuity, a common exam in clinical practice. All 20 subjects completed the Snellen test before and after a sham tDCS testing day and before and after an anodal tDCS testing day. The order of stimulation and the hemisphere stimulated (left or right) were counterbalanced across subjects.

Figure 4 shows that subjects scored higher on the Snellen test of central visual acuity after the lateral application of anodal tDCS compared with before anodal tDCS (pre versus post percent change, mean \pm SEM, $21.8\% \pm 9.2\%$; main effect of time on the logarithm of the minimal angle of resolution [logMAR] score, $p = 0.003$). Our sham condition allowed us to control for practice effects. We found that despite mild trend-level practice effects in the sham condition (mean \pm SEM, $7.2\% \pm 5.7\%$; main effect of time on logMAR score, $p = 0.06$), the anodal tDCS induced significantly greater behavioral gains relative to the sham condition, evidenced by a stimulation \times time interaction on logMAR score ($p = 0.04$). Accounting for practice effects, the stimulation boosted subjects' logMAR score by approximately 14.6%. An individual-subject analysis showed that all but two subjects had 20/20 vision (i.e., logMAR = 0) or better in both eyes, consistent with previous work with young adults [21] (see the Supplemental Information for results with these two subjects excluded). Despite the excellent vision of our subjects, the majority of subjects improved with tDCS (14 out of 20), correctly reading an additional 1.2 letters on average (accounting for practice effects) after the anodal stimulation. Individuals with the poorest eyesight experienced the largest stimulation-induced gains, evidenced by a significant subject-wise correlation ($p = 0.005$). If our findings generalize to individuals with clinical-grade vision deficits, the findings of experiment 4 suggest that those with the largest deficits may show the largest benefit of anodal tDCS. However, the true therapeutic utility of this tDCS protocol will require clinical research with patient populations.

Finally, in experiment 5, we tested whether the improvements in acuity following tDCS co-occurred with improvements in contrast sensitivity, given the close link between these visual functions [22–24]. Experiment 5 was identical to experiment 4, except that we used a two-interval forced choice task with a Bayesian adaptive procedure to estimate subjects' contrast sensitivity function across a range of spatial frequencies (0.5–20 cycles per degree [cpd]) (see the Supplemental Experimental Procedures for details). We found that anodal stimulation had an effect on mean contrast sensitivity, but only for contralaterally presented grating stimuli at high spatial frequencies (see Figure S1 and Table S1). This was demonstrated by an interaction between time and stimulation for contralateral ($p = 0.001$) but not ipsilateral stimuli ($p = 0.65$). Parsing this interaction revealed an improvement across time (pre versus post) in the anodal condition ($p = 0.001$) but not the sham ($p = 0.56$). Further, within the anodal condition, we observed a time \times frequency interaction ($p = 0.01$), driven by changes at spatial frequencies

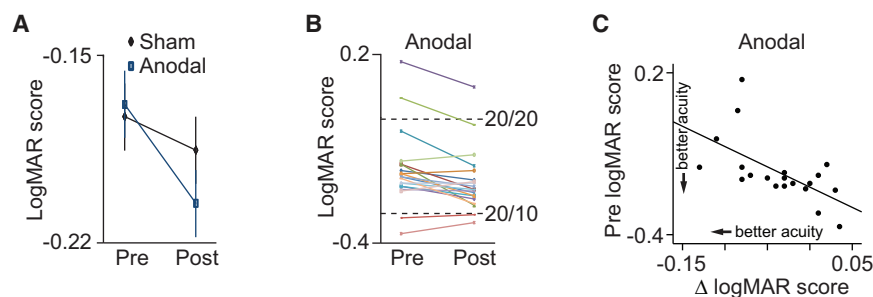


Figure 4. Results from Experiment 4

(A) Mean logarithm of the minimal angle of resolution (logMAR) scores from the Snellen eye chart before (pre) and after (post) sham and anodal visual cortex tDCS at 2.0 mA intensity. (B) Individual-subject data show the change in logMAR score before and after anodal tDCS. (C) Scatterplot showing the relationship between a subject's score on the Snellen test before anodal stimulation (pre logMAR score) and their improvement following anodal stimulation (i.e., post minus pre logMAR score). Smaller logMAR scores reflect better performance (i.e., more letters read correctly). See also Table S1 for the results of the statistical analyses in their entirety.

greater than 7 cpd (p 's < 0.03). These results converge with those from experiment 1 by showing that occipitoparietal tDCS can have a hemifield-selective influence on the high spatial frequency contrast sensitivity thresholds in the parafovea. These results add to previous work [10, 25] and confirm overlapping function between contrast sensitivity and visual acuity [22–24].

DISCUSSION

Our demonstration that anodal tDCS of occipitoparietal visual cortex improves spatial vision may seem counterintuitive, because this type of stimulation does not target the specific neurons that code for the line segments in the vernier acuity task or the letters on the Snellen chart. One might expect tDCS to increase both the noise and the signal to the same degree, given that anodal stimulation increases baseline firing rates in the absence of stimuli [20]. However, the present effects of tDCS could be accounted for in at least two ways. First, tDCS may have increased the gain for stimuli presented contralateral to the stimulation, consistent with our observation that the vernier stimuli elicited more vigorous electrophysiological responses following anodal stimulation and attenuated responses following cathodal stimulation. Second, the broad stimulating effects of anodal tDCS may have increased stochastic resonance. By increasing the baseline level of activity in the visual system under the anodal electrode, the signal-to-noise ratio may have been effectively increased because the addition of higher-amplitude white noise to this nonlinear neural system can improve processing [26]. In contrast, cathodal stimulation reduces activity levels, and the intrinsic stochastic resonance in the system, reducing the signal-to-noise ratio. Stochastic resonance has been shown to make a variety of neural systems more sensitive signal processors, and our anodal tDCS protocol may induce just such beneficial noise. We believe that these competing explanations can be distinguished by experiments that combine direct-current stimulation with recordings from neurons in animal models.

Here we found tDCS effects on spatial vision that last for over an hour, with large, immediate improvements in acuity (see Figure S2). How do we reconcile our results with previous work that found small effects of tDCS on the visual system that disappeared within 10 min of the end of stimulation [10, 27]? We see the electrode montage as the largest difference between the present and previous work. We stimulated occipitoparietal cortex using a distant cheek location for the other electrode. Previous

work placed one electrode over the occipital pole or over the fifth visual area (V5) and the other at the top of the head (central zenith electrode in the 10/20 system [Cz]), resulting in modest effects that lasted only a few minutes after stimulation ceased, possibly due to opposing effects induced by the electrode at Cz [20]. Because the cathodal and anodal electrodes push and pull activity levels in opposite directions, we will need experiments to verify that the electrode placements in previous work result in the short and counterintuitive effects compared to the effects observed here.

To increase the applicability of the occipitoparietal tDCS protocol as a potential therapeutic treatment, it will be necessary for future work to more extensively explore the tDCS parameter space. Lengthening stimulation duration, increasing the focality of current flow, and conducting repeated stimulation sessions with optimal spacing intervals [28] are methods that may generate longer-lasting improvements in spatial vision. Finally, our psychophysical manipulations tested vernier acuity at locations in the parafoveal belt using a brief stimulus presentation. It will be useful for future work to determine whether occipitoparietal stimulation influences processing in the fovea (<0.06°) and periphery (>5°) with prolonged viewing durations while tracking eye movements. Forthcoming work that addresses the above questions will significantly improve our understanding of our occipitoparietal tDCS method and determine its value for applications outside the laboratory.

SUPPLEMENTAL INFORMATION

Supplemental Information includes Supplemental Results and Discussion, Supplemental Experimental Procedures, two figures, and one table and can be found with this article online at <http://dx.doi.org/10.1016/j.cub.2016.05.019>.

AUTHOR CONTRIBUTIONS

R.M.G.R., W.X., and L.J.M. conducted the experiments and the analyses. R.M.G.R. and G.F.W. designed the experiments. R.M.G.R. and G.F.W. wrote the paper. All authors approved the final version of this report.

ACKNOWLEDGMENTS

This work was supported by grants from the NIH (R01-EY019882, R01-EY025275, P30-EY08126, T32-EY007135, F31-MH102042). We thank the reviewers and Randolph Blake for helpful comments. We thank Kevin Dieter for technical assistance in designing the psychophysical procedure

for experiment 5. Subjects gave informed written consent to procedures approved by the Vanderbilt University Institutional Review Board and were compensated at a rate of \$10/hr for their time.

Received: November 6, 2015

Revised: April 15, 2016

Accepted: May 5, 2016

Published: June 30, 2016

REFERENCES

- Hamill, M.B., and Koch, D.D. (1996). Refractive surgery—the cutting edge. *Nat. Med.* 2, 740–741.
- Palmer, S.E. (1999). *Vision Science: Photons to Phenomenology* (Bradford Books/MIT Press).
- Dolgin, E. (2015). The myopia boom. *Nature* 519, 276–278.
- Dutton, G.N. (2003). Cognitive vision, its disorders and differential diagnosis in adults and children: knowing where and what things are. *Eye (Lond.)* 17, 289–304.
- Deveau, J., Ozer, D.J., and Seitz, A.R. (2014). Improved vision and on-field performance in baseball through perceptual learning. *Curr. Biol.* 24, R146–R147.
- Sagi, D. (2011). Perceptual learning in vision research. *Vision Res.* 51, 1552–1566.
- Antal, A., Varga, E.T., Kincses, T.Z., Nitsche, M.A., and Paulus, W. (2004). Oscillatory brain activity and transcranial direct current stimulation in humans. *Neuroreport* 15, 1307–1310.
- Plow, E.B., Obretenova, S.N., Jackson, M.L., and Merabet, L.B. (2012). Temporal profile of functional visual rehabilitative outcomes modulated by transcranial direct current stimulation. *Neuromodulation* 15, 367–373.
- Spiegel, D.P., Byblow, W.D., Hess, R.F., and Thompson, B. (2013). Anodal transcranial direct current stimulation transiently improves contrast sensitivity and normalizes visual cortex activation in individuals with amblyopia. *Neurorehabil. Neural Repair* 27, 760–769.
- Antal, A., Nitsche, M.A., and Paulus, W. (2001). External modulation of visual perception in humans. *Neuroreport* 12, 3553–3555.
- Lavidor, M., and Walsh, V. (2004). The nature of foveal representation. *Nat. Rev. Neurosci.* 5, 729–735.
- Reinhart, R.M.G., and Woodman, G.F. (2014). Causal control of medial-frontal cortex governs electrophysiological and behavioral indices of performance monitoring and learning. *J. Neurosci.* 34, 4214–4227.
- Reinhart, R.M.G., and Woodman, G.F. (2015). Enhancing long-term memory with stimulation tunes visual attention in one trial. *Proc. Natl. Acad. Sci. USA* 112, 625–630.
- Reinhart, R.M.G., Zhu, J., Park, S., and Woodman, G.F. (2015). Medial-frontal stimulation enhances learning in schizophrenia by restoring prediction error signaling. *J. Neurosci.* 35, 12232–12240.
- Reinhart, R.M.G., Zhu, J., Park, S., and Woodman, G.F. (2015). Synchronizing theta oscillations with direct-current stimulation strengthens adaptive control in the human brain. *Proc. Natl. Acad. Sci. USA* 112, 9448–9453.
- Baker, T.Y., and Bryan, G.B. (1912). Errors of observation. In *Proceedings of the Optical Convention* (Hodder and Stroughton), pp. 252–263.
- Berry, R.N. (1948). Quantitative relations among vernier, real depth, and stereoscopic depth acuities. *J. Exp. Psychol.* 38, 708–721.
- Westheimer, G., and McKee, S.P. (1977). Spatial configurations for visual hyperacuity. *Vision Res.* 17, 941–947.
- Luck, S.J., and Hillyard, S.A. (1990). Electrophysiological evidence for parallel and serial processing during visual search. *Percept. Psychophys.* 48, 603–617.
- Bindman, L.J., Lippold, O.C.J., and Redfearn, J.W.T. (1962). Long-lasting changes in the level of the electrical activity of the cerebral cortex produced by polarizing currents. *Nature* 196, 584–585.
- Li, R.W., Brown, B., Edwards, M.H., Ngo, C.V., Chat, S.W., and Levi, D.M. (2012). Reduced sampling efficiency causes degraded vernier hyperacuity with normal aging: vernier acuity in position noise. *Sci. Rep.* 2, 300.
- Hawkins, A.S., Szlyk, J.P., Ardickas, Z., Alexander, K.R., and Wilensky, J.T. (2003). Comparison of contrast sensitivity, visual acuity, and Humphrey visual field testing in patients with glaucoma. *J. Glaucoma* 12, 134–138.
- Hashemi, H., Khabazkhoob, M., Jafarzadehpour, E., Emamian, M.H., Shariati, M., and Fotouhi, A. (2012). Contrast sensitivity evaluation in a population-based study in Shahroud, Iran. *Ophthalmology* 119, 541–546.
- Kromer, R., Serbecic, N., Krastel, H., and Beutelspacher, S.C. (2014). Comparison of VEP with contrast sensitivity and other measurements of central visual function. *Acta Ophthalmol.* 92, e141–e146.
- Kraft, A., Roehmel, J., Olma, M.C., Schmidt, S., Irlbacher, K., and Brandt, S.A. (2010). Transcranial direct current stimulation affects visual perception measured by threshold perimetry. *Exp. Brain Res.* 207, 283–290.
- McDonnell, M.D., and Ward, L.M. (2011). The benefits of noise in neural systems: bridging theory and experiment. *Nat. Rev. Neurosci.* 12, 415–426.
- Antal, A., Nitsche, M.A., Kruse, W., Kincses, T.Z., Hoffmann, K.P., and Paulus, W. (2004). Direct current stimulation over V5 enhances visuomotor coordination by improving motion perception in humans. *J. Cogn. Neurosci.* 16, 521–527.
- Goldsworthy, M.R., Pitcher, J.B., and Ridding, M.C. (2015). Spaced noninvasive brain stimulation: prospects for inducing long-lasting human cortical plasticity. *Neurorehabil. Neural Repair* 29, 714–721.

Current Biology, Volume 26

Supplemental Information

**Electrical Stimulation of Visual Cortex
Can Immediately Improve Spatial Vision**

Robert M.G. Reinhart, Wenxi Xiao, Laura J. McClenahan, and Geoffrey F. Woodman

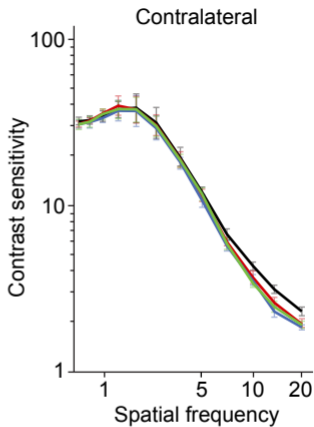
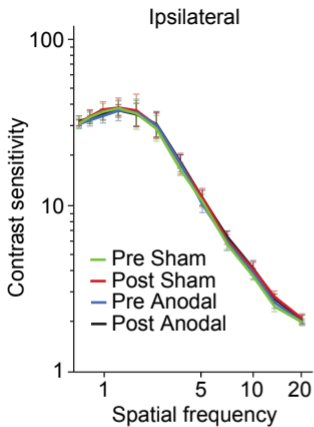


Figure S1

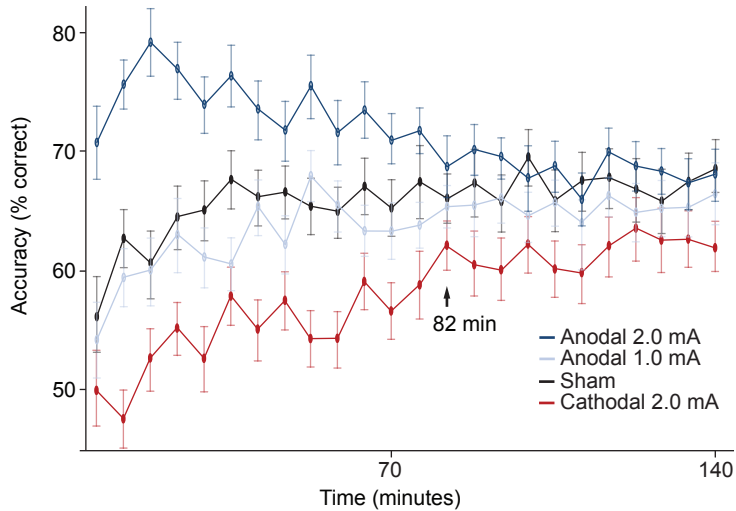


Figure S2

Supplemental Figure Legends

Figure S1. Results from Experiment 5. Contrast sensitivity as a function of spatial frequency (cycles per degree) before (Pre) and after (Post) the sham and anodal visual cortex tDCS. The data are sorted based on trials in which stimuli appeared in the ipsilateral (left panel) or contralateral (right panel) visual hemifields with respect to the location of stimulation. Error bars are ± 1 standard error of the mean. Figure S1 is related to the Experimental Design and the Supplemental Experimental Design.

Figure S2. Duration of transcranial direct-current stimulation effects during the vernier acuity task from Experiments 1-2. Mean performance accuracy (in percent correct) for stimuli appearing contralateral to tDCS application, collapsed across levels of vernier offset (2.2', 4.4', 6.6'), and sorted into 48-trial wide bins over the full 140-minute (or 2.3-hour) recording session from Experiments 1-2. Results from the 2.0 mA anodal (dark blue), 1.0 mA anodal (pale blue), sham (black), and 2.0 mA cathodal (red) conditions are shown based on the tDCS montage targeting visual cortex. The arrow marks the time interval (82 minutes from the start of the task) in which the stimulation conditions appear to converge. Error bars are ± 1 standard error of the mean. Figure S2 is related to the Discussion and the Supplemental Results and Discussion.

Table S1. Statistical results from Experiments 1, 2, 4, and 5.

Experiment 1	
	main effects of intensity
	2.0 vs. 1.5 vs. 1 mA, contralateral
RT	$F(2,38) = 4.645, d = 0.69, p = 0.016$
accuracy	$F(2,38) = 3.373, d = 0.59, p = 0.046$
	2.0 vs. 1.0 mA, contralateral
RT	$F(1,19) = 7.877, d = 0.91, p = 0.011$
accuracy	$F(1,19) = 4.570, d = 0.69, p = 0.046$
	2.0 vs 1.5 mA, contralateral
RT	$F(1,19) = 5.861, d = 0.78, p = 0.026$
accuracy	$F(1,19) = 4.945, d = 0.72, p = 0.038$
	2.0 vs. 1.5 vs. 1 mA, ipsilateral
RT	$F(2,38) = 0.425, d = 0.21, p = 0.647$
accuracy	$F(2,38) = 0.079, d = 0.09, p = 0.917$
	stimulation x location x intensity interactions
	contralateral
RT	$F(2,18) = 0.066, d = 0.08, p = 0.932$
accuracy	$F(2,18) = 0.233, d = 0.15, p = 0.793$
	ipsilateral
RT	$F(2,18) = 1.489, d = 0.30, p = 0.253$
accuracy	$F(2,18) = 0.048, d = 0.06, p = 0.950$
	main effects of intensity
	2.0 vs. 1.5 vs. 1 mA, contralateral
P1 amplitude	$F(2,38) = 3.400, d = 0.59, p = 0.053$
N1 amplitude	$F(2,38) = 6.295, d = 0.81, p = 0.010$
	2.0 vs. 1.0 mA, contralateral
P1 amplitude	$F(1,19) = 4.731, d = 0.70, p = 0.042$
N1 amplitude	$F(1,19) = 6.945, d = 0.85, p = 0.016$
	1.5 vs 1.0 mA, contralateral
P1 amplitude	$F(1,19) = 1.579, d = 0.40, p = 0.224$
N1 amplitude	$F(1,19) = 0.092, d = 0.09, p = 0.765$
	2.0 vs. 1.5 vs. 1 mA, ipsilateral
P1 amplitude	$F(2,38) = 0.479, d = 0.22, p = 0.619$
N1 amplitude	$F(2,38) = 0.087, d = 0.09, p = 0.901$
	1.5 vs 1.0 mA, ipsilateral
P1 amplitude	$F(1,19) = 0.469, d = 0.22, p = 0.502$
N1 amplitude	$F(1,19) = 0.012, d = 0.03, p = 0.913$
Experiment 2	
	main effects of stimulation
RT	2.0 mA vs. sham, contralateral
accuracy	$F(1,19) = 5.502, d = 0.76, p = 0.030$
	2.0 mA vs. sham, ipsilateral
RT	$F(1,19) = 0.003, d = 0.01, p = 0.956$
accuracy	$F(1,19) = 0.517, d = 0.23, p = 0.481$

Table S1

	2.0 mA vs. sham, contralateral
P1 amplitude	$F(1,19) = 1.494, d = 0.39, p = 0.236$
N1 amplitude	$F(1,19) = 5.367, d = 0.75, p = 0.032$
	2.0 mA vs. sham, ipsilateral
P1 amplitude	$F(1,19) = 0.017, d = 0.04, p = 0.897$
N1 amplitude	$F(1,19) = 0.025, d = 0.05, p = 0.877$
Experiment 4	
	main effect of time
	pre vs. post, anodal
logMAR	$F(1,19) = 11.862, d = 1.11, p = 0.003$
	pre vs. post, sham
logMAR	$F(1,19) = 3.788, d = 0.63, p = 0.067$
	stimulation x time interaction
logMAR	$F(1,19) = 4.500, d = 0.68, p = 0.047$
	subject-wise correlation
logMAR	$r(1,19) = -0.603, p = 0.005$
Experiment 5	
	stimulation x time interaction
	contralateral
contrast sensitivity	$F(1,19) = 16.003, d = 1.29, p = 0.001$
	ipsilateral
contrast sensitivity	$F(1,19) = 0.205, d = 0.14, p = 0.656$
	Main effect of time
	anodal, contralateral
contrast sensitivity	$F(1,19) = 16.316, d = 1.31, p = 0.001$
	sham, contralateral
contrast sensitivity	$F(1,19) = 0.351, d = 0.19, p = 0.561$
	anodal, ipsilateral
contrast sensitivity	$F(1,19) = 0.538, d = 0.23, p = 0.472$
	sham, ipsilateral
contrast sensitivity	$F(1,19) = 0.525, d = 0.23, p = 0.477$
	Time x frequency interaction
	anodal, contralateral
contrast sensitivity	$F(11,209) = 3.290, d = 0.58, p = 0.013$
	sham, contralateral
contrast	$F(11,209) = 0.107, d = 0.10, p = 0.763$

Table S1

sensitivity	
	anodal, ipsilateral
contrast sensitivity	$F(11,209) = 1.145, d = 0.34, p = 0.321$
	sham, ipsilateral
contrast sensitivity	$F(11,209) = 0.296, d = 0.17, p = 0.685$
	main effect of time
	anodal, contralateral
	frequency 0.50
contrast sensitivity	$F(1,19) = 2.178, d = 0.47, p = 0.156$
	frequency 0.69
contrast sensitivity	$F(1,19) = 0.064, d = 0.08, p = 0.804$
	frequency 0.97
contrast sensitivity	$F(1,19) = 0.192, d = 0.14, p = 0.666$
	frequency 1.36
contrast sensitivity	$F(1,19) = 0.087, d = 0.09, p = 0.772$
	frequency 1.91
contrast sensitivity	$F(1,19) = 2.879, d = 0.55, p = 0.106$
	frequency 2.67
contrast sensitivity	$F(1,19) = 2.527, d = 0.51, p = 0.128$
	frequency 3.73
contrast sensitivity	$F(1,19) = 1.926, d = 0.45, p = 0.181$
	frequency 5.22
contrast sensitivity	$F(1,19) = 1.722, d = 0.42, p = 0.205$
	frequency 7.31
contrast sensitivity	$F(1,19) = 5.623, d = 0.76, p = 0.028$
	frequency 10.22
contrast sensitivity	$F(1,19) = 10.556, d = 1.05, p = 0.004$
	frequency 14.30
contrast sensitivity	$F(1,19) = 9.517, d = 1.00, p = 0.006$
	frequency 20.00
contrast sensitivity	$F(1,19) = 13.252, d = 1.18, p = 0.002$

Table S1

Supplemental Experimental Procedures

Subjects

There were 100 different subjects who participated across five experiments (Experiment 1, $N = 20$, 11 women, mean age \pm SEM, 22.0 ± 0.9 ; Experiment 2, $N = 20$, 7 women, 25.3 ± 1.3 ; Experiment 3, $N = 20$, 13 women, 23.1 ± 1.2 ; Experiment 4, $N = 20$, 10 women, 22.4 ± 1.3 ; Experiment 5, $N = 20$, 6 women, 20.4 ± 1.8). All subjects self reported having normal color vision and normal or corrected-to-normal visual acuity. Subjects gave informed written consent to procedures approved by the Vanderbilt University Institutional Review Board and were compensated at a rate of \$10 per hour for their time. We had 6 subjects voluntarily withdraw from Experiment 1, and 3 subjects from Experiment 3. In addition, 2 subjects from Experiment 1, and 1 subject from Experiment 2 were removed due to excessive eye movements (eye movement measurement and rejection criteria are described below).

Stimuli and Procedure

Vernier Acuity Task. The vernier acuity task was in Experiments 1-3. An example of the sequence of events on each trial is shown in **Figure 1B**. The fixation point was presented for 1000 ms prior to the onset of the vernier stimuli. The vernier stimuli were then presented for 54 ms. Immediately after the offset of the vernier stimuli, a random visual noise mask was presented for 200 ms. Subjects pressed one of two buttons on a handheld gamepad to indicate whether the top line was to the right or left of the bottom line. Trial-by-trial feedback was presented for 1000ms following the registration of each response. The inter-trial interval was 1000-1200 ms, randomly jittered with a rectangular distribution. Vernier acuity is also known as hyperacuity because resolution at the fovea is less than the width of the dendritic tree of a photoreceptor [S1-S3]. We randomly varied the displacement of the two lines between 2.2, 4.4, and 6.6 arc minutes of gap offset, with the two line segments centered 5° of visual angle in the left or right visual field.

Stimuli were viewed on a gray background (54.3 cd/m^2) from a distance of 85 cm. A black fixation cross ($<0.01 \text{ cd/m}^2$, $0.4^\circ \times 0.4^\circ$ of visual angle) was visible throughout each trial. The vernier stimuli were two vertical line segments. One vertical line was presented above the other. Each of the two vertical line segments subtended 0.44° height \times 0.1° width of visual angle, centered 5° in the periphery (i.e., a location in the parafoveal belt) [S4]. The two lines were separated by a vertical gap of $8.8'$, and the upper line was displaced $2.2'$, $4.4'$, or $6.6'$ to the left or right of the lower line.

The vernier stimuli appeared to the left of fixation on half of the trials and to the right on the remainder, with the two types randomly interleaved across trials. Across all trials, the three gap offsets were randomly sampled with equal probability (33.3%), and the displacement to the left or right of the lower line was also equiprobable (50%). The visual noise mask was a $1.4^\circ \times 1.4^\circ$ square. The mask was centered on the location of the vernier stimuli. The visual noise mask was generated by randomly selecting the luminance of each cell of a 130×130 matrix with replacement.

Subjects were instructed to press one button using a handheld gamepad if the upper line was displaced to the left of the lower line, and a second button if the upper line was displaced to the right of the lower line. The duration, eccentricity, and masking of the vernier stimuli allowed us to avoid ceiling effects and keep overall performance at approximately 70%, consistent with previous work [S5]. The trial-by-trial feedback was a centrally presented outline of a circle (0.88° diameter, 0.13° thick) or cross (0.88° length, 0.13° thick), presented for 1000 ms immediately following each response, with the meaning of these symbols (i.e., correct versus incorrect) randomized across days and subjects. Each subject was given 96 practice trials. The task consisted of 1,152 trials with 30-second breaks every 100 trials.

Snellen Acuity Task. The Snellen acuity task was used in Experiment 4. We chose to use the Snellen chart so that we could generalize our findings from the vernier acuity task to a standard measure of visual acuity used outside the laboratory. The chart has letters of different sizes arranged from largest at the top to smallest at the bottom. Subjects read through the chart using one eye at a time. Subjects viewed the letters from a distance of 6 meters (or 20 feet). Based on this viewing distance and the reference standard (known today as 20/20), the 8th row of letters from the top of the chart consisted of letters subtending an angle of 5° with each letter part subtending 1° . Subjects started at the top of the chart and read each letter aloud to an experimenter who scored their performance. The Snellen exam was

conducted in a quiet, well-illuminated room with a full 20-foot lane (i.e., no mirrors necessary). Eleven subjects had corrected-to-normal visual acuity and used contacts or eyeglasses during the Snellen task. Two subjects who self-reported having correct-to-normal visual acuity had Snellen acuity slightly below 20/20. However, when we reran all analyses with these two low-acuity subjects removed from the sample, all results remained significant, including the acuity improvement observed between pre versus post time points in the anodal condition (main effect of time on logMAR score $F_{(1, 17)} = 16.347$, $d = 1.31$, $p = 0.001$), the time (pre versus post) x condition (sham versus anodal) interaction ($F_{(1, 17)} = 4.991$, $d = 0.72$, $p = 0.039$), and the subject-wise correlation between Snellen acuity at baseline and the stimulation-induced improvement in Snellen acuity ($r_{(1,17)} = -0.493$, $p = 0.038$).

Contrast sensitivity. In Experiment 5, we investigated the effects of the visual cortex stimulation on contrast perception by examining subjects' contrast sensitivity function (CSF). We implemented the quick CSF (qCSF) method, which provides an assessment of the complete shape of the CSF using a Bayesian adaptive simulation procedure [S6]. The rapid measurement of CSF allowed us to avoid bias in the results related to fatigue given the time-consuming nature of traditional CSF measurement, and obtain data immediately after electrical stimulation during which the impact of the stimulation was found to be strongest (see **Figure S1** and see **Table S1** for the results of the statistical analyses of Experiment 5).

Experiment 5 used a two interval forced choice target detection task. We changed the display on a 13-inch color CRT monitor (65-Hz refresh rate) to monochromatic, with 10-bit gray scale resolution, and linearized luminance values via a lookup table [S7]. Stimuli were Gaussian-windowed sinusoidal gratings, oriented $\pm 45^\circ$ from vertical, randomly interleaved across trials to the left or right of central fixation (5° eccentricity), rendered on a 400 x 400 pixel grid, subtending $5.6^\circ \times 5.6^\circ$, and viewed binocularly at roughly 80.5 cm in dim light. There were 12 possible grating spatial frequencies spaced log linearly from 0.5 to 20 cycles per degree (cpd), and 60 possible grating contrasts spaced log linearly from 0.1 to 100%. The stimulus sequence started with the presentation of a central fixation cross (500 ms), followed by a target-grating stimulus (130 ms). The target coincided with one of two consecutive auditory tones (500 and 1000 Hz, 130 ms). The auditory tones informed subjects of the two possible time intervals in which a grating target could appear and reduced stimulus uncertainty, which has been shown to affect CSF measurement, especially in the high-frequency region [S8]. Subjects pressed one button if they detected the target in the first interval, and a second button if they detected the target in the second interval.

The qCSF method uses the truncated log-parabola to characterize the CSF with four parameters (i.e., peak sensitivity or gain, peak spatial frequency, bandwidth in octaves, and low-frequency sensitivity truncation level) [S6]. A four dimensional probability density function is used to assign probabilities for combinations of the parameters. The spatial frequency and contrast of the stimulus on each trial is determined by the probability density function, which is updated with Bayes rule based on the subjects' response from the previous trial. From each qCSF measurement, the expectation value of the contrast sensitivity at individual spatial frequencies was estimated from the four-dimensional probability density function that was obtained at the end of 100 trials in each qCSF measurement, as described by Lesmes et al. (2010). This procedure calculates the most probable contrast sensitivity value for each spatial frequency. The individual contrast sensitivity values for 12 spatial frequencies between 0.5 and 20 cpd were analyzed.

Experimental Design

All experiments began with 20 minutes of transcranial direct-current stimulation (tDCS) applied over visual cortex (Experiments 1, 2, 4, and 5) or motor cortex (Experiment 3). Immediately following, subjects performed the vernier acuity task (Experiments 1-3), Snellen acuity task (Experiment 4), or contrast sensitivity task (Experiment 5) while we measured their behavior (Experiments 1-5) and electrical brain activity (Experiments 1-2). All experiments had a within-subjects design. That is, each subject completed all of the stimulation conditions to remove individual differences being confounded with the effects of stimulation.

In Experiment 1, we stimulated visual cortex with anodal tDCS and examined the effects of the stimulation on the electrophysiology and behavior during the vernier acuity task. We varied stimulation intensity across three levels (1.0 mA, 1.5 mA, and 2.0 mA anodal) administered across three separate testing days, with order randomized for each subject. Our goal was to determine the stimulation intensity that resulted in the maximum improvement in behavioral performance. After establishing that 2.0 mA of stimulation was maximally effective, we focused on this stimulation intensity and compared it with the sham control conditions in subsequent experiments.

In Experiment 2, we stimulated visual cortex with cathodal tDCS and examined the effects of stimulation on the electrophysiology and behavior during the vernier acuity task. Two different stimulation conditions (2.0 mA cathodal and a sham baseline) were administered across two separate testing days, order counterbalanced across subjects. In Experiment 3, we stimulated motor cortex with anodal tDCS and examined the effects of stimulation on behavioral metrics from the vernier acuity task. Two different stimulation conditions (2.0 mA anodal and sham baseline) were administered across two separate testing days, order counterbalanced across subjects. In Experiment 4, we stimulated visual cortex with anodal tDCS and examined the effects of stimulation on the Snellen acuity task. Snellen acuity scores were collected before and after the 2.0 mA anodal stimulation on one day, and before and after the baseline sham stimulation on another day. In Experiment 5, we stimulated visual cortex with anodal tDCS and examined the effects of stimulation on contrast perception. Contrast sensitivity function values were collected before and after the 2.0 mA anodal stimulation on one day, and before and after the baseline sham stimulation on another day, order counterbalanced across subjects. All experiments counterbalanced the hemisphere being stimulated across subjects, and tested for effects of hemisphere, although none were found, indicating symmetry of the stimulation effects across hemispheres. In all experiments, testing immediately followed the electrical stimulation.

Transcranial Direct-Current Stimulation

Apparatus and Procedure. The tDCS was administered using a battery driven, constant current stimulator (Mind Alive Inc., Alberta, Canada) and pair of conductive rubber electrodes (active: 19.25 cm² reference: 52 cm²). The electrodes were placed in saline-soaked sponges and held in place by a headband. Current was applied for 20 min over the left and right hemispheres (counterbalanced across subjects) of visual cortex (site P1 and P2 of the International 10-20 System) in Experiments 1, 2, 4, and 5, and over the left and right hemispheres (counterbalanced across subjects) of motor cortex (site C3 and C4) in Experiment 3. In Experiments 1, 3, 4, and 5 the anodal electrode on the head was paired with a cathodal electrode centered over the ipsilateral cheek to avoid confounding effects from other brain regions [S9, S10]. The direction of current was reversed in Experiment 2, such that the cathodal electrode was located on the head and the anodal electrode was over the ipsilateral cheek. Specifically, the cheek electrode was placed diagonally, 3 cm from the cheilion (lip corner at rest) along an imaginary line connecting the cheilion to the ipsilateral condyion (palpable when the jaw is moved) (**Figure 1A**).

Stimulation intensity varied across three levels (1.0 mA, 1.5 mA, and 2.0 mA) in Experiment 1, and was fixed at 2.0 mA in Experiments 2-5. Comparable stimulation protocols have been shown to cause effects lasting from 90 min [S11] up to 5 hr [S10]. The time interval between testing days was greater than 48 hours to minimize potential carryover effects related to repeated brain stimulation exposure [S12]. In Experiments 2-5, the sham tDCS condition followed the same procedure as the active tDCS, but stimulation only lasted 30 seconds, ramping up and down at the beginning and end of the 20-minute period. This sham procedure results in the same tingling and itching sensations associated with active tDCS. All subjects confirmed experiencing a mild tingling or itching sensation during the sham condition, and subjects were unable to distinguish between sham and active stimulation, as we discuss next.

We took two measures to ensure that subjects' expectations about the experimental procedures did not bias the results. First, subjects were blind to the intensity (Experiment 1) or presence (Experiments 2-5) of stimulation. Blinding was confirmed through a series of debriefing questions. Specifically, after each testing day, subjects completed a safety questionnaire [S13] and visual analog scale [S14], which included questions regarding attention, concentration, mood, vision, headache, fatigue, and skin sensations under the tDCS electrodes. We found that the scores from these ratings did not significantly differ between stimulation conditions in Experiments 1-5 ($F_s < 1.243$, $p_s > 0.280$). In addition, after the final day of testing, all subjects were directly asked to guess on which testing days they had received the various stimulation intensities (Experiment 1) or active versus sham stimulation (Experiments 2-5). Overall, subjects were near chance at detecting the proper intensity (33%) or presence (50%) of stimulation (Experiment 1: hit rate 25%; Experiment 2: hit rate 45%, Experiment 3: hit rate 55%; Experiment 4: hit rate 55%; Experiment 5: hit rate 50%). When we sorted the subjects based on those who guessed correctly versus incorrectly on this debriefing question, we found the same pattern of results for both groups across all of the experiments, and no significant differences as a function of response group. Second, to rule out potential confounding factors related to the order in which stimulation was presented, we examined whether stimulation order was introducing bias on our dependent variables. We found no interaction between stimulation order and the factors used in our statistical tests, including stimulation (i.e., active versus sham), stimulation intensity, stimulation location, target laterality, difficulty level, or time on any of our measures from Experiment 1 ($F_s < 1.1203$, $p_s > 0.325$), Experiment 2 ($F_s < 2.045$, $p_s >$

0.111), Experiment 3 ($F_s < 1.702$, $p_s > 0.200$), Experiment 4 ($F_s < 0.468$, $p_s > 0.582$), or Experiment 5 ($F_s < 2.214$, $p_s > 0.171$) verifying the effectiveness of the order randomization method we used across subjects.

Current-flow Modeling. To maximize stimulation of the targeted regions, tDCS electrode montages were configured and optimized based on current-flow modeling (HD-Target, HD-Explore, Soterix Medical, NY) and previous research methods [S15]. Current-flow models used a finite element method to compute the distribution of the electric field into a standard adult head model. The modeling results shown in **Figures 1A, 2A, and 3A** show the estimated electric field orientation and intensity in targeted areas, based on the selected montages. As with our previous modeling work [S10, S15-S17], we do not regard these estimates as definitive solutions about the exact location of current flow during stimulation. However, these models do serve as working hypotheses for how the current flow is spatially distributed through the brain, and offer potential target locations for investigators using techniques in human neuroimaging or animal neurophysiology.

Electrophysiology

For Experiments 1-3, the testing was conducted in a double-walled sound-attenuating electrically shielded isolation booth to eliminate external sources of electrical noise. For Experiments 1 and 2, the raw electroencephalogram (EEG) was recorded (250 Hz sampling rate, 0.01 to 100-Hz bandpass filter) with an SA Instrumentation amplifier using non-polarizable tin electrodes embedded in an elastic cap (Electrocap International, Eaton, OH). The recording electrodes were arrayed according to the International 10/20 System (Fz, Cz, Pz, F3/F4, C3/C4, P3/P4, PO3/PO4, T3/T4, T5/T6, O1/O2) including 2 nonstandard sites (OL, midway between O1 and T5; and OR, midway between O2 and T6). Signals were referenced online to the right mastoid electrode and re-referenced offline to the average of the left and the right mastoids [S18]. Horizontal eye position was monitored by recording electrooculogram (EOG) from bipolar electrodes placed at the outer canthi of each eye. Vertical eye position and blinks were monitored with bipolar electrodes placed above and below the left eye. Peri-orbital electrodes detected eye movements and a two-step ocular artifact rejection method was used [S19], resulting in the removal of 2 subjects from Experiment 1, and 1 subject from Experiment 2 for excessive eye movements (either $> 25\%$ of individual trials rejected or any residual systematic eye movement that resulted in HEOG voltage deflections $> 3.2 \mu\text{V}$, corresponding to an ocular deviation of $\pm 0.1^\circ$).

Data Analysis

Event-related Potentials. To confirm that tDCS was changing how the visual system was processing information early in the processing stream, we recorded the early event-related potential (ERP) components known to index sensory and perceptual processing [S20]. The EEG was time-locked to the onset of the vernier stimuli, baseline corrected to the period from -200 to 0 ms prior to stimulus onset, and displayed from -100 to 250 ms relative to stimulus onset. The P1 and N1 components were measured from lateral occipital electrodes (OL/R) where these components are maximal. We quantified mean amplitude using 50-ms long measurement windows centered on the peak of the P1 and N1 waveforms (P1: 75 to 125 ms; N1: 140 to 190 ms) [S20]. Grand average waveforms were 35 Hz low-pass filtered for presentation purposes, but all analyses were performed on unfiltered waveforms. Voltage topographies were calculated using spherical-spline interpolation [S21].

Snellen Acuity. Our measure of Snellen acuity was calculated using the letter assignment scoring method where subjects earned credit for correctly naming individual letters on the Snellen chart, as opposed to line assignment method which requires correctly reading a complete line of the letters. Letter-based scoring allowed us to overcome several disadvantages of Snellen charts. For example, letter-based scoring allows measurement of visual acuity on a finer scale. In contrast, by using line assignment with variable letters per line, a change in acuity of one letter can yield a change of vision of an entire line. Second, because of the lack of standardized progression between lines, Snellen acuity is difficult to examine statistically using line-based scoring. To remedy this, we obtained letter-based scores and converted them to the standard geometric notation for expressing visual acuity, called the logarithm of the minimal angle of resolution (LogMAR). LogMAR is the logarithm to the base 10 of the angular subtense of the stroke widths at 6 meters (or 20 feet). The minimal angle of resolution (or MAR) is the width of one bar on a Snellen E. In logMAR notation, lower scores denote better acuity, and vision becomes worse as the logMAR values increases. A logMAR of 0 is equivalent to 20/20 vision.

In addition to choosing a more rigorous scoring method, we made efforts to minimize the underlying variability in the Snellen chart measurement. To do this, our Snellen acuity experiment was a within-subjects design, and consisted of pre- and post-stimulation Snellen testing on both the active tDCS day and the sham tDCS day. This allowed us to capture the test-retest variability on each day and reduce spurious statistical results when calculating the effects of stimulation on Snellen acuity. It is important to note that the Snellen test is common in clinical practice, not vision research. Our primary reason for using the Snellen chart was not because of its scientific merits as a rigorous experimental assessment, but rather, because the Snellen chart is widely used among clinicians to measure visual acuity, and thus provides the opportunity to test the real-world applicability of the visual cortex stimulation protocol that we used in this study. Moreover, despite its shortcomings, the measurement of Snellen acuity has provided a critical data point for comparison with other systematic measurements of visual field function in basic and clinical research [S22-S31].

Statistical Analysis. Across the five experiments, we computed analyses of variance (ANOVAs) using the within-subjects factors of stimulation (anodal vs. sham or cathodal vs. sham), stimulation intensity (1.0 mA vs. 1.5 mA vs. 2.0 mA), stimulation location (left hemisphere vs. right hemisphere), stimulus laterality (contralateral vs. ipsilateral), vernier offset difficulty (2.2', 4.4', 6.6'), and time (pre stimulation vs. post stimulation) on our dependent measures, including RT, accuracy, logMAR score, contrast sensitivity, and the amplitudes of P1 and N1 components. Trials were binned according to the location of vernier stimuli with respect to the hemisphere that had been electrically stimulated (i.e., ipsilateral or contralateral). Also, trials were binned according to the level of the task difficulty determined by the gap-offset distance between vernier stimuli (i.e., 2.2', 4.4', or 6.6'). Where appropriate, follow up ANOVAs were conducted to test specific preplanned hypotheses. P-values were adjusted using the Greenhouse-Geisser epsilon correction for nonsphericity when this assumption was violated [S32]. Finally, we calculated Cohen's d effect size estimates [S33] for each analysis to facilitate comparisons between studies and promote replication.

Supplemental Results and Discussion

We found that tDCS over visual cortex modulated vernier acuity for well over 1 hour. **Figure S2** shows the within-session dynamics of mean accuracy in the vernier acuity task from Experiments 1-2. These data were obtained from trials in which stimuli appeared contralateral to tDCS application, collapsed across the difficulty levels of vernier offset (i.e., 2.2', 4.4', 6.6'), and sorted into 48-trial wide bins across the full 2.3-hour recording session. We calculated two-tailed t-tests at each time bin between stimulation conditions. To determine when the tDCS effects wore off, we searched the behavioral time series for time bins where there were no significant ($p > 0.05$) between-condition differences, provided they were followed by at least 5 consecutive non-significant time bins (i.e., roughly 30 minutes of task) to ensure the stability of performance over time.

For the anodal tDCS of Experiment 1, we found that relative to the 1.0 mA intensity, accuracy improvements following 2.0 mA stimulation were largest during the first hour of the task, but that these advantages in vernier acuity were no longer statistically significant after approximately 82 minutes. A similar result was found when comparing the 2.0 mA anodal condition of Experiment 1 to the baseline sham condition of Experiment 2. In addition, the behavioral dynamics following the 2.0 mA cathodal tDCS also converged with the baseline sham condition after approximately 82 minutes from the start of the task. However, after this 82-minute period, we observed changes in behavior that significantly differed from baseline, suggesting that subjects may not have fully recovered from the cathodal stimulation effects by the end of the experiment. It seems likely that these long lasting after effects of tDCS may still be influencing behavior at the end of our recordings, and that significantly longer follow-up experiments will be needed to observe when the benefits of anodal tDCS and the costs of cathodal tDCS truly disappear. Importantly, these results demonstrate that a single dose of 20 minutes of anodal tDCS over visual cortex is powerful enough to produce spatial resolution benefits in the parafoveal belt (i.e., 5° eccentricity) lasting well over 1 hour in healthy young adults with normal vision, highlighting the translational potential of the brain stimulation protocol we have developed. This is striking given that previous studies using tDCS of primary visual cortex [S34-S38] have tended to show mostly online effects (i.e., during stimulation) with relatively transient offline effects (i.e., < 10 min following stimulation), including those for contrast sensitivity [S34], motion detection thresholds [S39] and perception of phosphenes [S37, S38]. In contrast, our results show far more enduring and lasting effects of visual perception offline. In addition, it is possible that the duration of the stimulation results on visual acuity may be greater for individuals with poorer vision, given our findings from Experiment 4 using the Snellen chart, and that repeated stimulation combined with behavioral training could offer more lasting benefits.

The duration findings allow us to address the possibility that occipitoparietal tDCS defocused subjects' vision during the 20-minute period of stimulation, resulting in a neural compensation and visual improvement, similar to enhancements in vision following time without refractive correction [40]. Defocus induced blur adaption has been reported to modify supra-threshold contrast sensitivity at multiple spatial frequencies, from 3.22 [S41], 8, 12 [S42], up to 25 cpd [S40], and for stimuli presented at the fovea and locations of the parafoveal nasal visual field (2°, 4°, 6°, 8°, 10°) with best-corrected distance vision [S43]. Adaptation changes in contrast sensitivity can influence letter acuity, and studies have found that changes in high contrast letter acuity following defocus adaptation ranges from two letters when adjusting to subjects' own myopic refractive error [S44] to approximately three lines while adapting to +2.50 D blur [S45]. Critically, the majority of these effects are observed online, and when aftereffects are examined they typically last approximately 5 minutes [S41]. By contrast, in the present study we found offline effects with significantly longer lasting improvements in vision. These data argue against the view that the tDCS-triggered improvements were due to defocus induced blur adaptation. Nonetheless, we believe this question requires future work with more definitive assessment techniques.

The results from Experiments 1 and 2 allow us to rule out several alternative explanations for the effects we observed. It is possible that the direct-current stimulation changed the deployment of visual-spatial attention, such that the focus of attention was biased toward the visual field contralateral to the stimulation [S46, S47]. However, if tDCS had biased attention in this way, then we should have observed the opposite pattern of effects ipsilateral to the stimulation, because capacity limits define mechanisms of attentional selection [S48]. For example, if tDCS worked like a spatial cue, resulting in a shift of visual-spatial attention into the left visual hemifield, then this benefit should improve processing for left visual field stimuli at the expense of processing right visual field stimuli. Contrary to this prediction, our results consistently showed effects contralateral to the tDCS, with no accompanying tradeoff for ipsilaterally presented stimuli. Previous work with the vernier task indicates that the absence of task-irrelevant distractors and the use of just two spatial locations for the vernier stimuli make it unlikely that attention would play a significant role in this task [S49, S50]. The next explanation that we can rule out is that tDCS changed the precision of spatial vision by altering pupil dilation and accommodation [S51]. However, if this had been the case, then we would not have observed effects in one hemifield but not the other. Thus, the present results and paradigm provide evidence that tDCS changed sensory-level activity in the cortex leading to a systematic modulation of the precision of spatial vision and are difficult to account for with alternative explanations based on attention, pupil dilation, or accommodation.

The electrophysiological evidence from Experiments 1-2 suggest the occipitoparietal tDCS induced changes in vernier acuity by augmenting early stages of neural information processing. In the main text, we focus on the two canonical visual evoked potentials (i.e., the P1 and N1) hypothesized to derive from extrastriate visual areas [20]. Here, we assess an even earlier component called the C1, which is typically observed between 65 and 90 ms poststimulus onset and thought to have neural generators in primary visual cortex [52-54]. We found no significant effects of anodal stimulation intensity on C1 amplitude in Experiment 1 (contralateral, $F_{(2, 38)} = 1.961$, $d = 0.45$, $p = 0.162$; ipsilateral, $F_{(2, 38)} = 0.297$, $d = 0.17$, $p = 0.714$), and no effect of cathodal stimulation on C1 amplitude in Experiment 2 (contralateral, $F_{(1, 19)} = 2.091$, $d = 0.46$, $p = 0.164$; ipsilateral, $F_{(1, 19)} = 1.316$, $d = 0.37$, $p = 0.266$). These results demonstrate the offline temporal specificity of the stimulation effects on the neural mechanisms of visual perceptual processing. The findings across Experiments 1-2 suggest that the behavioral changes we observed in visual acuity following occipitoparietal tDCS were due to the stimulation having changed an intermediate stage of processing likely involving regions of extrastriate visual cortex.

In Experiment 3 we wanted to determine if the improvements in spatial vision that we measured in Experiment 1 were specific to stimulation of visual cortex, or would be observed following any lateralized stimulation of the human brain. For example, perhaps the lateralized stimulation increases arousal of the subjects or results in subjects expecting to perform better contralateral to the stimulation (i.e., demand characteristics).

In Experiment 3 we stimulated motor cortex of subjects (left or right, counterbalanced across subjects) with 2.0 mA of anodal stimulation or sham (see **Figure 3A**). All subjects performed both conditions with order counterbalanced. We found that subjects simply responded with greater overall speed regardless of the visual field the stimuli (main effect of stimulation on RTs: $F_{(1, 19)} = 11.031$, $d = 1.07$, $p = 0.004$) (see **Figure 3B**). Further, unlike the spatially mapped pattern of performance observed after visual cortex tDCS, we observed behavioral RT advantages for stimuli presented in both hemifields (contralateral: $F_{(1, 19)} = 4.704$, $d = 0.70$, $p = 0.043$; ipsilateral: $F_{(1, 19)} = 4.704$, $d = 0.70$, $p = 0.043$).

$_{19} = 4.490, d = 0.68, p = 0.047$) and no stimulation x target laterality interaction ($F_{(1, 19)} = 0.014, d = 0.03, p = 0.906$). Third, there was no improvement in accuracy ($F_{(1, 19)} = 1.506, d = 0.39, p = 0.235$) (see **Figure 3C**). If anything we observed a slight decline in accuracy across conditions, suggesting that motor cortex stimulation resulted in a speed-accuracy tradeoff. These results show that the improvements we observed previously were specific to tDCS of visual cortex.

The present study provides new information to a growing body of work focused on developing interventions for the remediation of visual deficits in patient populations. Studies using behavioral training have shown that practice can boost vernier acuity [S25, S55] contrast sensitivity, and letter recognition [S22] in adult amblyopia, with effects lasting for months [S22, S25, S30] to a year or more [S22, S28]. Similarly, action videogame training in amblyopia patients has been shown to result in a range of improved spatial and temporal visual functions including visual acuity [S56]. In addition to behavioral interventions, the use of non-invasive brain stimulation techniques for the treatment of vision disorders, such as amblyopia is rapidly developing [S57-S59], and tDCS is particularly attractive due to its low cost and portability. Specifically, tDCS in conjunction with training protocols offers advantages such as shortened training time, which without stimulation often requires thousands of trials over days to weeks of practice, as well as generating more potent and enduring perceptual improvements. For example, visual benefits in contrast sensitivity and uncorrected visual acuity (a gain of 0.15 logMAR) following 2 months of perceptual training can be reduced to only 2 weeks of training when coupled with noninvasive brain stimulation [S60]. Moreover, improvements in visual acuity and stereopsis in adults with amblyopia have been shown to be more pronounced and longer lasting following 2 weeks of anodal tDCS over primary visual cortex combined with videogame-based dichoptic perceptual training as compared with dichoptic training alone [S61]. Anodal tDCS of visual cortex coupled with behavioral training has also been reported to enhance the rehabilitation of visual field deficits after stroke [S62, S63]. The present findings raise the possibility for further capitalizing on the experience-dependent plasticity mediating performance- and stimulation-induced visual enhancements, and for optimizing interventions with the goal of speeding recovery following visual cortical damage and rescuing function in patients with vision disorders. In addition, the contrast sensitivity improvements measured in Experiment 5 with 50% contrast suggest that acuity benefits could be even larger than the 15% improvement we found here under 100% contrast with Vernier stimuli.

Supplemental References

- S1. Baker, T.Y., and Bryan, G.B. (1912). Errors of observation. In *Proceedings of the Optical Convention*, H.a. Stroughton, ed. (London).
- S2. Berry, R.N. (1948). Quantitative relations among vernier, real depth, and stereoscopic depth acuities. *Journal of Experimental Psychology* 38, 708-721.
- S3. Westheimer, G., and McKee, S.P. (1977). Spatial configurations for visual hyperacuity. *Vision Research* 17, 941-947.
- S4. Schira, M.M., Tyler, C.W., Breakspear, M., and Spehar, B. (2009). The foveal confluence in human visual cortex. *Journal of Neuroscience* 29, 9050-9058.
- S5. Yeshurun, Y., and Carrasco, M. (1999). Spatial attention improves performance in spatial resolution tasks. *Vision Research* 39, 293-305.
- S6. Lesmes, L.A., Lu, Z.-L., Baek, J., and Albright, T.D. (2010). Bayesian adaptive estimation of the contrast sensitivity function: The quick CSF method. *Journal of Vision* 10, 1-21.
- S7. Li, X., Lu, Z.L., Xu, P., Jin, J., and Zhou, Y. (2003). Generating high gray-level resolution monochrome displays with conventional computer graphics cards and color monitors. *Journal of Neuroscience Methods* 130, 9-18.
- S8. Woods, R.L. (1996). Spatial frequency dependent observer bias in the measurement of contrast sensitivity. *Ophthalmic and Physiological Optics* 16, 513-519.
- S9. Tseng, P., Hsu, T.-Y., Chang, C.-F., Tzeng, O., Hung, D., Muggleton, N., Walsh, V., Liang, W.-K., Cheng, S.-k., and Juan, C.-H. (2012). Unleashing Potential: Transcranial direct current stimulation over the right posterior parietal cortex improves change detection in low-performing individuals. *Journal of Neuroscience* 32, 10554-10561.
- S10. Reinhart, R.M.G., and Woodman, G.F. (2014). Causal control of medial-frontal cortex governs electrophysiological and behavioral indices of performance monitoring and learning. *Journal of Neuroscience* 34, 4214-4227.
- S11. Nitsche, M., and Paulus, W. (2001). Sustained excitability elevations induced by transcranial DC motor cortex stimulation in humans. *Neurology* 57, 1899-1901.
- S12. Monte-Silva, K., Kuo, M.F., Hessenthaler, S., Fresnoza, S., Liebetanz, D., Paulus, W., and Nitsche, M.A. (2013). Induction of late LTP-like plasticity in the human motor cortex by repeated non-invasive brain stimulation. *Brain Stimulation* 6, 424-432.
- S13. Poreisz, C., Boros, K., Antal, A., and Paulus, W. (2007). Safety aspects of transcranial direct current stimulation concerning healthy subjects and patients. *Brain Research Bulletin* 72, 208-214.
- S14. Gandiga, P., Hummel, F., and Cohen, L. (2006). Transcranial DC stimulation (tDCS): A tool for double-blind sham-controlled clinical studies in brain stimulation. *Clinical Neurophysiology* 117, 845-850.
- S15. Reinhart, R.M.G., and Woodman, G.F. (2015). Enhancing long-term memory with stimulation tunes visual attention in one trial. *Proceedings of the National Academy of Sciences of the USA* 112, 625-630.
- S16. Reinhart, R.M.G., Zhu, J., Park, S., and Woodman, G.F. (2015). Medial-frontal stimulation enhances learning in schizophrenia by restoring prediction-error signaling. *Journal of Neuroscience* 35, 12232-12240.
- S17. Reinhart, R.M.G., Zhu, J., Park, S., and Woodman, G.F. (2015). Synchronizing theta oscillations with direct-current stimulation strengthens adaptive control in the human brain. *Proceedings of the National Academy of Sciences of the USA* 112, 9448-9453.
- S18. Nunez, P.L., and Srinivasan, R. (2006). *Electric fields of the brain: The neurophysics of EEG*, 2nd Edition, (Oxford: Oxford University Press, Inc.).
- S19. Woodman, G.F., and Luck, S.J. (2003). Serial deployment of attention during visual search. *Journal of Experimental Psychology: Human Perception and Performance* 29, 121-138.
- S20. Luck, S.J., and Hillyard, S.A. (1990). Electrophysiological evidence for parallel and serial processing during visual search. *Perception & Psychophysics* 48, 603-617.
- S21. Perrin, F., Pernier, J., Bertrand, O., and Echallier, J.F. (1989). Spherical splines for scalp potential and current density mapping. *Electroencephalography and Clinical Neurophysiology* 72, 184-187.
- S22. Polat, U., Ma-Naim, T., Belkin, M., and Sagi, D. (2004). Improving vision in adult amblyopia by perceptual learning. *Proceedings of the National Academy of Sciences of the USA* 101, 6692-6697.
- S23. Li, R.W., and Levi, D.M. (2004). Characterizing the mechanisms of improvement for position discrimination in adult amblyopia. *Journal of Vision* 4, 476-487.

- S24. Fronius, M., Chopovska, Y., Nolden, J., Loudon, S.E., Luchtenberg, M., Zubcov, A., and Pepler, L. (2006). Occlusion treatment for amblyopia: assessing the performance of the electronic occlusion dose monitor. *Strabismus* 14, 65-70.
- S25. Levi, D.M., Polat, U., and Hu, Y.S. (1997). Improvement in Vernier acuity in adults with amblyopia. Practice makes better. *Investigative Ophthalmology & Visual Science* 38, 1493-1510.
- S26. Li, R.W., Young, K.G., Hoenig, P., and Levi, D.M. (2005). Perceptual learning improves visual performance in juvenile amblyopia. *Investigative Ophthalmology & Visual Science* 46, 3161-3168.
- S27. Li, R.W., Provost, A., and Levi, D.M. (2007). Extended perceptual learning results in substantial recovery of positional acuity and visual acuity in juvenile amblyopia. *Investigative Ophthalmology & Visual Science* 48, 5046-5051.
- S28. Zhou, Y., Huang, C., Xu, P., Tao, L., Qiu, Z., Li, X., and Lu, Z.L. (2006). Perceptual learning improves contrast sensitivity and visual acuity in adults with anisometropic amblyopia. *Vision Research* 46, 739-750.
- S29. Huang, C.B., Zhou, Y., and Lu, Z.L. (2008). Broad bandwidth of perceptual learning in the visual system of adults with anisometropic amblyopia. *Proceedings of the National Academy of Sciences of the USA* 105, 4068-4073.
- S30. Chen, P.L., Chen, J.T., Fu, J.J., Chien, K.H., and Lu, D.W. (2008). A pilot study of anisometropic amblyopia improved in adults and children by perceptual learning: An alternative treatment to patching. *Ophthalmic and Physiological Optics* 28, 422-428.
- S31. Levi, D.M., and Li, R.W. (2009). Perceptual learning as a potential treatment for amblyopia: a mini-review. *Vision Research* 49, 2535-2549.
- S32. Jennings, J.R., and Wood, C.C. (1976). The e-adjustment procedure for repeated-measures analyses of variance. *Psychophysiology* 13, 277-278.
- S33. Cohen, J. (1988). *Statistical Power Analysis for the Behavioral Sciences*, 2nd Edition, (New Jersey: Lawrence Erlbaum Associates).
- S34. Antal, A., Nitsche, M.A., and Paulus, W. (2001). External modulation of visual perception in humans. *Neuroreport* 16, 3553-3555.
- S35. Accornero, N., Li Voti, P., La Riccia, M., and Gregori, B. (2007). Visual evoked potentials modulation during direct current cortical polarization. *Experimental Brain Research* 178, 261-266.
- S36. Antal, A., Varga, E.T., Kincses, T.Z., Nitsche, M.A., and Paulus, W. (2004). Oscillatory brain activity and transcranial direct current stimulation in humans. *NeuroReport* 15, 1307-1310.
- S37. Antal, A., Kincses, T., Nitsche, M., and Paulus, W. (2003). Manipulation of phosphene thresholds by transcranial direct current stimulation in man. *Experimental Brain Research* 150, 375-378.
- S38. Antal, A., Kincses, T.Z., Nitsche, M.A., and Paulus, W. (2003). Modulation of moving phosphene thresholds by transcranial direct current stimulation of V1 in humans. *Neuropsychologia* 41, 1802-1807.
- S39. Antal, A., Nitsche, M.A., Kruse, W., Kincses, T.Z., Hoffman, K.P., and Paulus, W. (2004). Direct current stimulation over V5 enhances visuo-motor coordination by improving motion perception in humans *Journal of Cognitive Neuroscience* 16, 521-527.
- S40. Mon-Williams, M., Tresilian, J.R., Strang, N.C., Kochhar, P., and Wann, J.P. (1998). Improving vision: neural compensation for optical defocus. *Proceedings of the Royal Society B: Biological Sciences* 265, 71-77.
- S41. Ohlendorf, A., and Schaeffel, F. (2009). Contrast adaptation induced by defocus – a possible error signal for emmetropization. *Vision Research* 49, 249-256.
- S42. Rajeev, N., and Metha, A. (2010). Enhanced contrast sensitivity confirms active compensation in blur adaptation. *Investigative Ophthalmology & Visual Science* 51, 1242-1246.
- S43. Mankowska, A., Aziz, K., Cufflin, M., Whitaker, D., and Mallen, E.A.H. (2012). Effect of blur adaptation on human parafoveal vision. *Investigative Ophthalmology & Visual Science* 53, 1145-1150.
- S44. Pesudovs, K., and Brennan, N.A. (1993). Decreased uncorrected vision after a period of distance fixation with spectacle wear. *Optometry & Vision Science* 70, 528-531.
- S45. George, S., and Rosenfield, M. (2004). Blur adaptation and myopia. *Optometry & Vision Science* 81, 543-547.
- S46. Yeshurun, Y., and Carrasco, M. (1998). Attention improves or impairs visual performance by enhancing spatial resolution. *Nature* 396, 72-75.
- S47. Anton-Erxleben, K., and Carrasco, M. (2013). Attentional enhancement of spatial resolution: linking behavioural and neurophysiological evidence. *Nature Reviews Neuroscience* 14, 188-200.

- S48. Mangun, G.R., and Hillyard, S.A. (1990). Allocation of visual attention to spatial location: Event-related brain potentials and detection performance. *Perception and Psychophysics* 47, 532-550.
- S49. Shiu, L., and Pashler, H. (1994). Negligible effect of spatial precuing on identification of single digits. *Journal of Experimental Psychology: Human Perception and Performance* 20, 1037-1054.
- S50. Shiu, L.P., and Pashler, H. (1995). Spatial attention and vernier acuity. *Vision Res* 35, 337-343.
- S51. Davson, H. (1990). *Physiology of the eye*, (London: The MacMillan Press Ltd).
- S52. Jeffreys, D.A., and Axford, J.G. (1972). Source locations of pattern-specific components of human visual evoked potentials. II: Components of extrastriate cortical origin. *Experimental Brain Research* 16, 22-40.
- S53. Clark, V.P., Fan, S., and Hillyard, S.A. (1995). Identification of early visually evoked potential generators by retinotopic and topographic analyses. *Human Brain Mapping* 2, 170-187.
- S54. Di Russo, F., Martinez, A., and Hillyard, S.A. (2003). Source analysis of event-related cortical activity during visuo-spatial attention. *Cerebral Cortex* 13, 486-499.
- S55. Levi, D.M., and Polat, U. (1996). Neural plasticity in adults with amblyopia. *Proceedings of the National Academy of Sciences of the USA* 93, 6830-6834.
- S56. Li, R.W., Ngo, C., Nguyen, J., and Levi, D.M. (2011). Video-game play induces plasticity in the visual system of adults with amblyopia. *Public Library of Sciences Biology* 9, e1001135.
- S57. Thompson, B., Mansouri, B., Koski, L., and Hess, R.F. (2008). Brain plasticity in the adult: modulation of function in amblyopia with rTMS. *Current Biology* 18, 1067-1071.
- S58. Spiegel, D.P., Byblow, W.D., Hess, R.F., and Thompson, B. (2013). Anodal transcranial direct current stimulation transiently improves contrast sensitivity and normalizes visual cortex activation in individuals with amblyopia. *Neurorehabilitation and Neural Repair* 27, 760-769.
- S59. Clavagnier, S., Thompson, B., and Hess, R.F. (2013). Long lasting effects of daily theta burst rTMS sessions in the human amblyopic cortex. *Brain Stimulation* 6, 860-867.
- S60. Camilleri, R., Pavan, A., Ghin, F., Battaglini, L., and Campana, G. (2014). Improvement of uncorrected visual acuity and contrast sensitivity with perceptual learning and transcranial random noise stimulation in individuals with mild myopia. *Frontiers in Psychology* 5, 1234.
- S61. Spiegel, D.P., Li, J., Hess, R.F., Byblow, W.D., Deng, D., Yu, M., and Thompson, B. (2013). Transcranial direct current stimulation enhances recovery of stereopsis in adults with amblyopia. *Neurotherapeutics* 10, 831-839.
- S62. Plow, E.B., Obretenova, S.N., Jackson, M.L., and Merabet, L.B. (2012). Temporal profile of functional visual rehabilitative outcomes modulated by transcranial direct current stimulation. *Neuromodulation* 15, 367-373.
- S63. Plow, E.B., Obretenova, S.N., Fregni, F., Pascual-Leone, A., and Merabet, L.B. (2012). Comparison of visual field training for hemianopia with active versus sham transcranial direct cortical stimulation. *Neurorehabilitation and Neural Repair* 26, 616-626.